Single Calcium Channel Behavior in Native Skeletal Muscle

ROBERT T. DIRKSEN and KURT G. BEAM

From the Department of Physiology, Colorado State University, Fort Collins, Colorado 80523

ABSTRACT The purpose of this study was to use whole-cell and cell-attached patches of cultured skeletal muscle myotubes to study the macroscopic and unitary behavior of voltage-dependent calcium channels under similar conditions. With 110 mM $BaCl_2$ as the charge carrier, two types of calcium channels with markedly different single-channel and macroscopic properties were found. One class was DHP-insensitive, had a single-channel conductance of ~ 9 pS, yielded ensembles that displayed an activation threshold near -40 mV, and activated and inactivated rapidly in a voltage-dependent manner (T current). The second class could only be well resolved in the presence of the DHP agonist Bay K 8644 (5 μM) and had a single-channel conductance of ~ 14 pS (L current). The 14-pS channel produced ensembles exhibiting a threshold of ~ -10 mV that activated slowly ($\tau_{act} \sim 20$ ms) and displayed little inactivation. Moreover, the DHP antagonist, (+)-PN 200–110 (10 μM), greatly increased the percentage of null sweeps seen with the 14-pS channel. The open probability versus voltage relationship of the 14-pS channel was fitted by a Boltzmann distribution with a $V_{P0.5} = 6.2$ mV and $k_P = 5.3$ mV. L current recorded from whole-cell experiments in the presence of 110 mM $BaCl_2$ + 5 μM Bay K 8644 displayed similar time- and voltage-dependent properties as ensembles of the 14-pS channel. Thus, these data are the first comparison under similar conditions of the single-channel and macroscopic properties of T current and L current in native skeletal muscle, and identify the 9- and 14-pS channels as the single-channel correlates of T current and L current, respectively.

INTRODUCTION

Voltage-dependent calcium channels play an essential role in the function of mammalian skeletal muscle. Thus, skeletal muscle dihydropyridine receptors (DH-PRs) have been postulated to serve a dual function: (a) to act as voltage sensors (Chandler, Rakowski, and Schneider, 1976) which provide the structural link between surface membrane depolarization and intracellular calcium release from the sarcoplasmic reticulum (Ríos and Brum, 1987; Adams, Tanabe, Mikami, Numa, and Beam, 1990); and (b) to produce a slow, voltage-dependent calcium conductance pathway (L current) (Donaldson and Beam, 1983; Beam, Knudson, and Powell, 1986;

Cognard, Lazdunski, and Romey, 1986a; Cognard, Romey, Galizzi, Fosset, and Lazdunski, 1986b). Moreover, potentiation of L current has been proposed to lead to enhanced contractile force upon tetanic stimulation (Sculptoreanu, Scheuer, and Catterall, 1993). Rapidly activating, noninactivating calcium currents distinct from L current have also been identified in frog (Arreola, Calvo, Garcia, and Sanchez, 1987; Cota and Stefani, 1986) and dysgenic mouse skeletal muscle, but are not detected in normal mouse skeletal muscle (Adams and Beam, 1989). In addition, a low-threshold, fast-activating, transient current (T current) that is insensitive to DHPs is also present in skeletal muscle obtained from rats (Cognard et al., 1986a,b; Beam and Knudson, 1988a,b) and mice (Beam et al., 1986; Beam and Knudson, 1988a; Gonoi and Hasegawa, 1988). T current is the predominant calcium current expressed in the first two weeks of postnatal development in rat skeletal muscle (Beam and Knudson, 1988b). Thus, T current has been suggested to influence pacemaker activity linked to spontaneous contractions of noninnervated muscle (Cognard et al., 1986a) and a variety of developmental processes such as myogenesis, elimination of redundant synapses, and gene transcription (Beam and Knudson, 1988a).

Unitary behavior due to calcium channel activity corresponding to L current and T current has been extensively studied in neuronal (Fox, Nowycky, and Tsien, 1987), cardiac (Nilius, Hess, Lansman, and Tsien, 1985; Cavalié, Pelzer, and Trautwein, 1986) and secretory (Armstrong and Eckert, 1987) tissues, but not in skeletal muscle. Moreover, some of the properties of macroscopic calcium currents in these other cell types differ in important respects (i.e., activation, inactivation, permeability, and modulation) from those of L current and T current observed in native skeletal muscle. Single-channel calcium currents attributable to L current have been recorded from either clonal skeletal muscle cell lines (Caffrey, Brown, and Schneider, 1987; Winegar and Lansman, 1990; Lansman, 1990), artificial planar lipid bilayers containing purified transverse tubules (T tubules) or DHPRs (Affolter and Coronado, 1985; Flockerzi, Oeken, Hofmann, Pelzer, Cavalié, and Trautwein, 1986; Smith, McKenna, Ma, Vilven, Vaghy, Schwartz, and Coronado, 1987; Hymel, Striessing, Glossmann, and Schindler, 1988; Ma and Coronado, 1988; Yatani, Imoto, Codina, Hamilton, Brown, and Birnbaumer, 1988; Ma, Mundiña-Weilenmann, Hosey, and Ríos, 1991; Mejía-Alvarez, Fill, and Stefani, 1991), or from nonmuscle cells transfected with the cDNA encoding the α_1 subunit of the skeletal muscle DHPR (Perez-Reyes, Kim, Lacerda, Horne, Wei, Rampe, Campbell, Brown, and Birnbaumer, 1989; Parent, Gopalakrishnan, Lacerda, and Brown, 1994). These studies, however, have produced conflicting results with regard to the presence or absence of subconductance states and the relationship between the voltage dependencies of single-channel open probability and whole-cell conductance of L current. It is unclear whether these discrepancies are due to differences in species, preparation, and/or the technique employed.

Unfortunately, measurements of unitary activity due to L current or T current in native adult skeletal muscle has heretofore been unsuccessful, presumably because T current disappears during postnatal development (Beam and Knudson, 1988b) and because the majority of L current channels/voltage sensors are present in the T tubules, deep within the muscle fiber (Fosset, Jaimovitch, Delpont, and Lazdunski, 1983). However, early during muscle development in vivo and in vitro, triads are

absent and excitation-contraction (E-C) coupling is thought to occur at peripheral junctions between the SR and sarcolemma (Franzini-Armstrong, Pincon-Raymond, and Rieger, 1991). Within the sarcolemma of these developing muscle cells are found groups of intramembrane particles (junctional tetrads) which are postulated to represent DHPRs (Block, Imagawa, Campbell, and Francini-Armstrong, 1988). This idea is supported by the absence of junctional tetrads in diaphragms and cultured skeletal muscle myotubes from dysgenic mice (Franzini-Armstrong et al., 1991), and their restoration by transfection with cDNA encoding the skeletal muscle DHPR (Takekura, Bennett, Tanabe, Beam, and Franzini-Armstrong, 1994). If junctional tetrads indeed represent DHPRs, developing muscle should be a suitable preparation for examining the single-channel properties of skeletal L current.

Thus, we have used the cell-attached patch clamp technique to monitor the unitary behavior of voltage-activated skeletal muscle calcium channels in their native environment. We report here two distinct voltage-dependent calcium channel conductances present in native skeletal muscle myotubes. One channel is DHP insensitive, has a low conductance (9 pS), and displays rapid, voltage-dependent activation and inactivation similar to that seen for T current recorded macroscopically. The other is a DHP-sensitive 14-pS channel, that produces a slowly activating and noninactivating (in 200 ms) ensemble, similar to macroscopic L current. L current and immobilization-resistant intramembrane charge movement were recorded under the same conditions used in the single-channel experiments in order allow a quantitative comparison with the average behavior of the 14-pS channel. Preliminary accounts of some of the results have appeared previously in abstract form (Dirksen, Tanabe, and Beam, 1993; Dirksen and Beam, 1994).

METHODS

Primary cultures of myotubes were prepared from skeletal muscle of newborn mice, as described previously (Beam and Knudson, 1988). All experiments were performed 7–11 d after the initial plating of myoblasts and were carried out at room temperature (20–22°C). Numerical figures are presented in the text and figures as mean ± SEM.

Single-Channel Measurements

Single-channel calcium currents were measured using the cell-attached mode of the patch clamp technique (Hamill, Marty, Neher, Sakmann, and Sigworth, 1981). Fire-polished borosilicate pipettes were coated with Sylgard (Dow-Corning, Midland, MI) and had resistances of 2–4 MΩ when filled with the pipette solution. Typically, seal resistances ranged from 20–100 GΩ. Currents were measured with an EPC-7 patch clamp amplifier (Medical Systems, Greenvale, NY), filtered at 1 kHz with an 8-pole Bessel filter (Frequency Devices, Inc., Haverhill, MA), and acquired at 10 kHz using an IDA Interface (INDEC Systems, Capitola, CA). Data were collected using the Basic-Fastlab (INDEC Systems, Capitola, CA) software and analyzed using a combination of pCLAMP (Axon Instruments, Foster City, CA) and an analysis program kindly provided by Dr. Don Campbell and modified by Aaron Beam.

Single-channel records were digitally corrected for leak and capacitative currents by subtracting from each record either the average of multiple sweeps without channel openings (null sweeps) or a double exponential that had been fitted to a null sweep. Ensemble averages were compiled by averaging all subtracted current records in a series. To calculate the potential across the patch membrane (cell resting potential minus pipette potential), resting potentials

were measured at the end of experiments by rupturing the cell-attached patch while in current clamp mode. Resting potentials averaged -59.0 ± 0.7 mV ($n = 28$). Thus, a value of -60 mV was assumed for the resting membrane potential in calculations of absolute patch potentials. All patches were either held at their resting potential (-60 mV) or 30 mV hyperpolarized to the resting potential (-90 mV). Single-channel openings and closings were determined with a 50% threshold crossing method. The amplitude of the open-channel current was taken as the average current between adjacent openings and closings. Mean open-current amplitudes were determined from Gaussian fits of either all-point current amplitude histograms (see Fig. 4) or amplitude histograms of single open events. Open-time durations were similarly measured, binned (at 0.5 ms), and fit with the sum of two exponentials (see Table I). In patches containing more than one channel (the majority of experiments), open-time durations were calculated only for single-channel openings from the zero-current level. Open probability (P_0) was calculated from the following equation:

$$P_0 = I/(N \cdot i),\tag{1}$$

where I is either the peak ensemble current at the end of the pulse (for weak depolarizations) or the peak ensemble tail current (for strong depolarizations), N is the observed maximum number of simultaneously open channels, and i is the single-channel current amplitude during the pulse or upon repolarization. Using this method, a maximum P_0 value of 0.19 (from nine different patches) was calculated. This value is similar to that reported previously for skeletal L-type calcium channels measured in the presence of DHP agonist (Ma et al., 1991; Mejía-Alvarez et al., 1991). P_0 values were normalized to their maximum values and fitted with a single Boltzmann distribution (see Fig. 7).

A large conductance channel distinct from channels producing L current and T current that appeared to be activated by increasing pipette suction (I_{str}) was often observed in myotubes. Similar to stretch-activated channels reported in guinea pig smooth muscle (Wellner and Isenberg, 1993) and mouse skeletal muscle (Franco and Lansman, 1990a,b), I_{str} exhibits a single-channel conductance ~ 20 pS in 110 mM $BaCl_2$. In addition, I_{str} is a relatively nonselective cation channel because it reversed near 0 mV with either 110 mM $BaCl_2$ or 150 mM NaCl in the pipette solution. This channel was easily distinguished from channels producing L current and T current due its large conductance, reversal potential, and openings persisting at negative potentials. Only experiments lacking activity attributable to I_{str} were analyzed in this study.

Macroscopic Ionic Currents

Macroscopic L current was recorded using the whole-cell variant of the patch clamp technique (Hamill et al., 1981). Pipettes were fabricated from borosilicate glass and had resistances of 1.8–2.2 MΩ when filled with the internal solution. Linear capacitative and leakage currents were determined by averaging the currents elicited by multiple (usually 10) 20-mV hyperpolarizing pulses from a holding potential of -80 mV. This control current was then scaled appropriately and used to correct test currents for linear components of capacitative and leakage currents. Electronic compensation was used to reduce the effective series resistance (usually to ≤ 1 MΩ) and the time constant for charging the linear cell capacitance to ≤ 0.5 ms. Cell capacitance was determined by integration of the capacity transient resulting from the control pulse and was used to normalize currents (pA/pF) or charge movements (nC/μF) obtained from different myotubes. Data were filtered at 2 kHz and sampled at 1 kHz. To measure macroscopic L current in isolation, a 1-s prepulse to -30 mV followed by a 25-ms repolarization to -50 mV (prepulse protocol) was used to inactivate T current.

The activation phase of macroscopic and ensemble currents were fitted by the following exponential function:

$$I(t) = I_\infty[1 - \exp(-t/\tau_{act})] \tag{2}$$

where $I(t)$ is the current at time t after the depolarization, I_∞ is the steady state current, and τ_{act} is the time constant of activation.

Intramembrane Charge Movement

Immobilization-resistant intramembrane charge movements were measured in whole-cell mode by a method described previously (Adams et al., 1990). Ionic currents due to voltage-dependent calcium channels were blocked by the addition of 0.5 mM $CdCl_2$ + 0.2 mM $LaCl_3$ to the extracellular recording solution (see Solutions). Voltage clamp command pulses were rounded with a time constant of 50–300 μs. The prepulse protocol preceded all test depolarizations in order to immobilize gating currents due to sodium and T-type calcium channels. The amount of charge moved by the test depolarization was obtained by integrating the transient of charge that moved outward after the onset of the test pulse (Q_{on}).

Solutions

For single-channel experiments, myotubes were bathed in a normal rodent Ringer solution consisting of (in millimolar): 145 NaCl, 5 KCl, 2 $CaCl_2$, 1 $MgCl_2$, and 10 HEPES (pH = 7.40 with NaOH). Cell-attached patch pipettes were filled with a solution consisting of (in millimolar): 110 $BaCl_2$, 0.003 tetrodotoxin, and 10 HEPES (pH = 7.40 with TEA-OH). For single-channel experiments on L current, 5 μM ($\pm$) Bay K 8644 (kindly supplied by Dr. A. Scriabine, Miles Laboratories, Inc., New Haven, CT) was also included in the pipette solution.

For measurements of macroscopic currents, the internal solution consisted of (in millimolar): 140 Cs-aspartate, 10 Cs_2-EGTA, 5 $MgCl_2$, and 10 HEPES (pH = 7.40 with CsOH). The external solution contained (in millimolar): 145 TEA-Cl, 10 $CaCl_2$, 0.003 TTX and 10 HEPES (pH = 7.40 with TEA-OH). Macroscopic L current was also measured in the presence of the aforementioned single-channel pipette solution. These external solutions were supplemented with 0.5 mM $CdCl_2$ + 0.2 mM $LaCl_3$ for experiments on intramembrane charge movement. The DHP antagonist, (+)-PN 200-110, was kindly provided by Drs. E. Rossi and A. Lindenmann of Sandoz Ltd. (Basel, Switzerland).

RESULTS

A 9-pS Calcium Channel Produces T Current

Fig. 1 shows unitary activity at two voltages of a low conductance calcium channel in a cell-attached patch of a cultured mouse skeletal muscle myotube. For each voltage, the patch was depolarized from the holding potential (−60 mV) to either −30 (*left*) or −20 mV (*right*) for 200 ms. In this and all subsequent figures, downward current deflections represent channel openings. Five representative, leak-subtracted sweeps for each voltage are displayed in the middle panel of Fig. 1. Ensemble averages of 120 (−30 mV) and 155 (−20 mV) individual leak subtracted sweeps for both voltages are shown at the bottom of Fig. 1. Similar to macroscopically recorded T current (Beam and Knudson, 1988a,b) ensembles of this low conductance channel activate at negative voltages and inactivate more rapidly at stronger depolarizations. Patches

were sometimes encountered which contained more than 10 channels (Fig. 2 *A*); the ensembles from these patches exhibited voltage dependence and kinetics of activation and inactivation identical to ensembles for single-channel patches. Thus, isolated channels and clustered channels displayed similar properties. The average single-channel current amplitude versus voltage relationship for the low conductance channel obtained from patches containing up to four channels is shown in Fig. 2 *B*. From a total of seven experiments, this channel had a single-channel conductance of 8.7 pS. Unitary activity of this 9-pS channel was unaffected by the DHP agonist Bay K 8644 (data not shown).
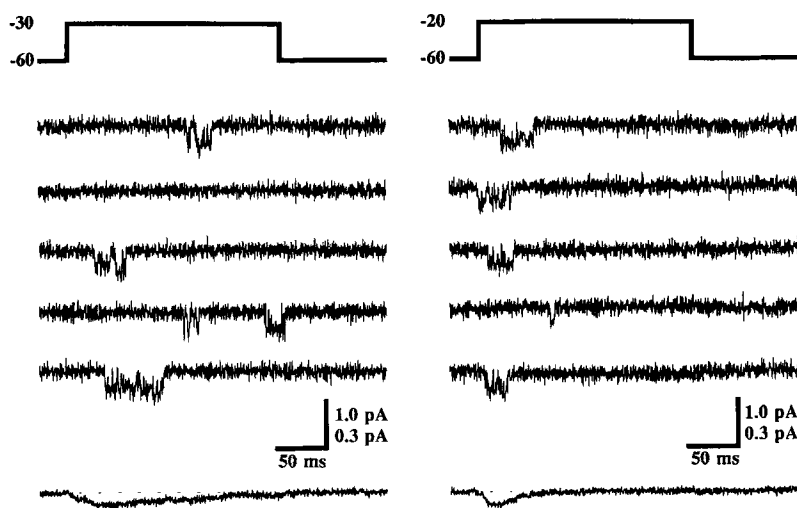

FIGURE 1.   Unitary activity of a low conductance calcium channel in developing mouse skeletal muscle. (*Top*) The voltage protocol consisted of 200-ms depolarizing pulses from the holding potential (−60 mV) to either −30 (*left*) or −20 mV (*right*). (*Middle*) Selected sweeps showing unitary activity of the low conductance calcium channel. In this and all subsequent figures of unitary activity, 110 mM Ba^{2+} was the charge carrier, leak and capacitative currents were subtracted as described in Methods, and downward deflections represent inward currents. The calculated open-channel levels at −30 and −20 mV were 0.46 and 0.37 pA, respectively. A single-channel conductance of 9.0 pS was calculated from this two-channel patch (calibrations: vertical = 2.0 pA; horizontal = 50 ms). (*Bottom*) Ensemble averages of 120 (*left*) and 155 (*right*) individual leak subtracted sweeps. (*Dotted line*) Zero-current level (calibrations: vertical = 0.5 pA; horizontal = 50 ms).

A 14-pS Calcium Channel Produces L Current

A larger conductance calcium channel, distinct from that producing T current, was also found in cultured myotubes (Figs. 3–7). Unitary activity of this channel in response to 200-ms depolarizations to two different potentials is shown in Fig. 3. In the presence of Bay K 8644 (5 μM), stronger depolarizations were required to open this larger conductance channel than the 9-pS channel. Openings of the larger

conductance channel were characterized by both brief and long durations, and often exhibited a bursting-type behavior. At times when the channel remained open at the end of the depolarization, single-channel tail currents were observed upon repolarization (Fig. 3, *arrows*). Ensemble averages displayed a slow time constant of activation (τ_{act}) at 20 mV (23.2 ± 4.9 ms, $n = 7$) and exhibited little inactivation during a 200-ms pulse. Ensembles from patches containing many channels (> 10) had kinetics and voltage dependence similar to those of ensembles of patches containing only a few channels (data not shown). Thus, as for the 9-pS channel, channel clustering does not appear to alter gating of the larger conductance channel.

Fig. 4, *A* and *B*, depict all-point amplitude histograms of leak subtracted currents
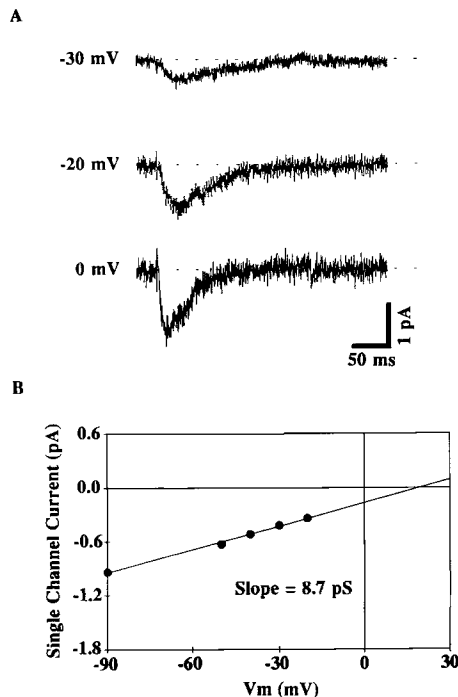

FIGURE 2. Voltage dependence of the low conductance channel. (*A*) Ensembles taken from a cell-attached patch containing more than 10 low conductance channels. Ensembles were elicited by 200-ms depolarizing pulses from the holding potential (-90 mV) to the potentials indicated to the left of each trace. Ensemble currents from patches with many channels activated and inactivated in a voltage-dependent manner similar to ensembles from patches containing 1–4 channels. (*Dotted line*) Zero-current level. (*B*) Average single-channel current versus voltage relationship tabulated from a total of seven different patches, with each patch containing up to four channels. Standard errors are smaller than symbol size. Unitary events of the low conductance channel could occasionally be detected at potentials as negative as -50 mV. A linear regression of the data ($R^2 = 0.9978$) revealed a single-channel conductance of 8.7 pS.

at two different test depolarizations (same patch as Fig. 3). The amplitude histograms were fit by the sum of either two (Fig. 4 *A*) or four (Fig. 4 *B*) Gaussian distributions. In both histograms, the large peak near 0 pA represents the current level when all channels were closed. At 0 mV, a second peak centered at -0.77 pA corresponded to the single open-channel current amplitude. No other significant conductance state was found at this voltage. At 20 mV, the Gaussian distribution had four peaks, occurring in multiples of ~ 0.48 pA, and proportionally favoring the lower amplitude peaks. The data of Fig. 4 suggest the presence of three identically conducting channels in the patch, and indicate the absence of intermediate conductances.

Unitary activity of the large conductance calcium channel was sensitive to the DHP

antagonist (+)-PN 200-110 (Fig. 5). In the absence of the antagonist (Fig. 5; *left*), unitary and ensemble behavior resembled those seen in Fig. 3. However, the addition of 10 μM (+)-PN 200-110, greatly increased the percentage of null sweeps (control = 30.7%; (+)-PN 200-110 = 96.9%) and blocked the development of a time-dependent inward ensemble current (Fig. 5 *B; right*). However, although rare, single-channel events in the presence of (+)-PN 200-110 DHP, were qualitatively similar to openings in the absence of the antagonist (see trace *4* in Fig. 5; *right*).

Open-time analysis of the large conductance channel is shown in Fig. 6. Fig. 6 *A* illustrates leak subtracted single-channel (*middle*) and ensemble (*bottom*) traces
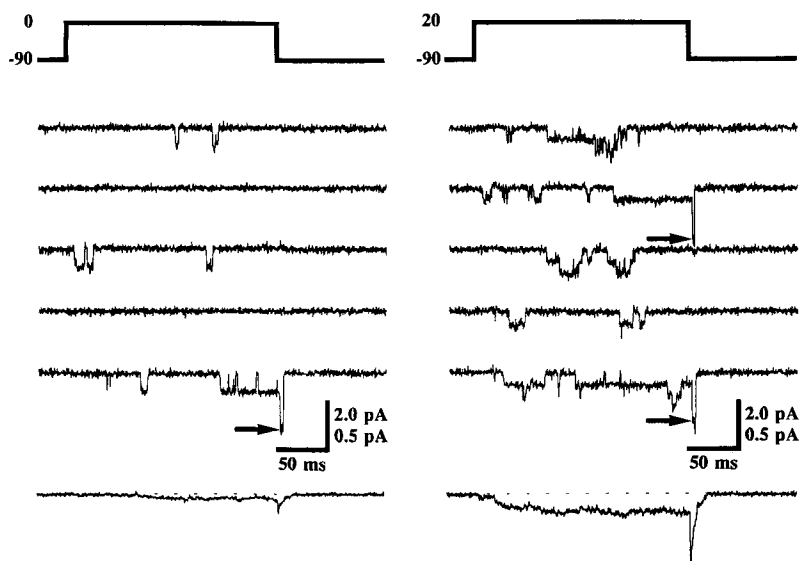

FIGURE 3. Unitary activity of a large conductance calcium channel in developing mouse skeletal muscle. (*Top*) The voltage protocol consisted of 200-ms depolarizing pulses from the holding potential (−90 mV) to either 0 (*left*) or 20 mV (*right*). (*Middle*) Selected sweeps of unitary activity of the large conductance calcium channel (calibrations: vertical = 2.0 pA; horizontal = 50 ms). For this and all subsequent experiments on the large conductance channel, 5 μM (±) Bay K 8644 was present in the pipette solution. Arrows indicate single-channel tail currents. (*Bottom*) Ensemble averages of 80 individual leak subtracted sweeps (calibrations: vertical = 0.5 pA; horizontal = 50 ms). For the test pulse to 20 mV, the ensemble had a τ_{act} = 26.1 ms. (*Dotted line*) Zero-current level.

resulting from 200-ms depolarizations from −90 to 0 mV. The amplitude histogram of all single open events (total = 825) obtained from a total of 140 similar sweeps is shown in Fig. 6 *B*. In this and eight other similar experiments, open-time histograms were best fit by the sum of two exponentials, with variable weights (Table I). A brief open time of ~2 ms was observed at all voltages, whereas the longer open time (~20–50 ms) varied considerably. Skeletal L-type calcium channels reconstituted into bilayers have also been shown to exhibit two open times under similar conditions (Ma et al., 1991). Thus, the voltage dependence, kinetics, DHP sensitivity, and open-time

analysis identify the unitary behavior of the larger conductance channel in cultured skeletal muscle myotubes as the single-channel correlate of L current.

The voltage dependencies of the single-channel current amplitude (i-V) and normalized open probability (NP_0 − V) of the large conductance channel are shown in Fig. 7. From a total of 11 experiments, the large conductance channel had a slope conductance of 13.8 pS (Fig. 7 A). The NP_0-V relationship of the large conductance channel was well fitted by a single Boltzmann distribution with a calculated $V_{P0.5}$ = 6.2 mV and k_P = 5.3 mV (Fig. 7 B).
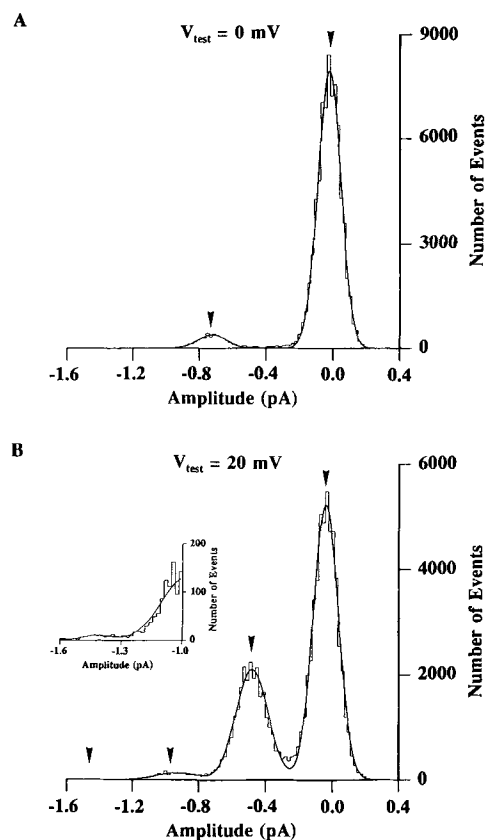

FIGURE 4. All-point amplitude histograms at 0 (A) and 20 mV (B) taken from the experiment shown in Fig. 3. Each histogram was constructed from either 39 (A) or 40 (B) consecutive leak subtracted traces. The smooth curves represent the best fit of the sum of two (A) or four (B) Gaussian distributions (*arrowheads*). The contribution of large current amplitude events (−1.6 to −1.0 pA) to the Gaussian fit at 20 mV are presented at an expanded scale in B (*inset*). The fitted parameters for central values (μ) and standard deviation (σ) were: (A) 0 mV; μ_1 = −0.034, σ_1 = 0.072, μ_2 = −0.770, and σ_2 = 0.091; (B) 20 mV; μ_1 = −0.047, σ_1 = 0.079, μ_2 = −0.512, σ_2 = 0.101, μ_3 = −0.990, σ_3 = 0.131, μ_4 = −1.479, and σ_4 = 0.111. The Gaussian distributions at 20 mV were represented by four peaks that occurred in multiples of ~0.477 pA indicating the presence of a total of three similarly conducting channels. A single-channel conductance of 14.5 pS was calculated from this three-channel patch using the combination of these and three similar histograms constructed from a total of five different voltages.

Effect of Single-Channel Recording Conditions on Macroscopic L Current

Although the single-channel behavior of the 14-pS channel qualitatively resembles macroscopic L current recorded from cultured skeletal muscle myotubes (Beam et al., 1986; Beam and Knudson, 1988*a*), some quantitative differences exist. For example, macroscopic L current activates three to four times more slowly than the ensembles

shown in Figs. 3, 5, and 6. In addition, the conductance versus voltage $(G\text{-}V)$ relationship of L current recorded macroscopically (Adams et al., 1990; García, Tanabe, and Beam, 1994) is shifted by $\sim +10$ mV compared to the $NP_0\text{-}V$ relationship shown in Fig. 7 B. Two likely reasons for these differences are the use of a different charge carrier (110 mM Ba^{2+} vs. 10 mM Ca^{2+}) and the presence of DHP agonist during the single-channel measurements. Thus, we measured whole cell L current under recording conditions like those used for the single-channel measurements (Figs. 8 and 10 A).
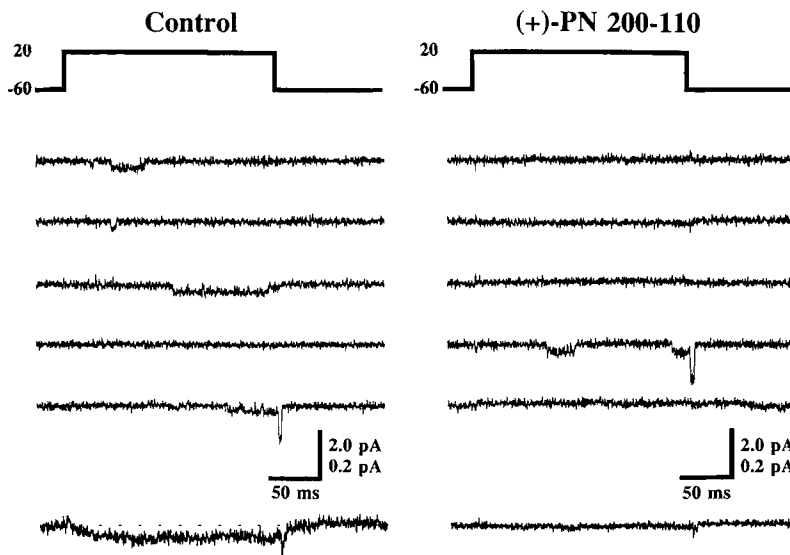

FIGURE 5. Unitary activity of the large conductance channel is sensitive to a DHP antagonist. Single-channel (*middle,* calibrations: vertical = 2.0 pA; horizontal = 50 ms) and ensemble (*bottom,* calibrations: vertical = 0.5 pA; horizontal = 50 ms) traces resulting from 200-ms depolarizations from the holding potential (-60 mV) to 20 mV in the absence (*left*) or presence (*right*) of 10 μM (+)-PN 200-110 added to the bath outside the pipette. The percentage of null sweeps was greatly increased in the presence of (+)-PN 200-110 (187 nulls/193 sweeps = 96.9%) compared to control (47 nulls/153 sweeps = 30.7%). The control ensemble (average of 80 sweeps) had a τ_{act} = 22.1 ms. (+)-PN 200-110 blocked the development of a time-dependent inward ensemble current (average of 80 sweeps). (*Dotted line*) Zero-current level.

Fig. 8 illustrates the effect of the single-channel recording conditions on the activation time constant of macroscopically recorded L current. In the absence of DHP, with 10 Ca^{2+} as charge carrier (Fig. 8 A, *left*), L current activates very slowly (τ_{act} = 72.3 ± 2.4 ms, n = 23, at 40 mV). After exchanging the extracellular solution for our single-channel pipette solution, L current increased in magnitude approximately threefold and the time constant of activation decreased approximately fourfold (Fig. 8 A; *right*). On average, the single-channel recording conditions
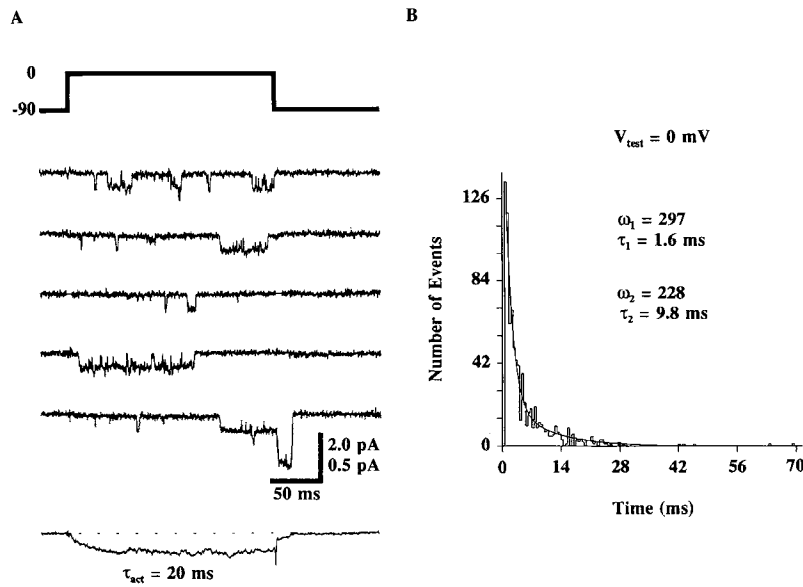
A   B

FIGURE 6.   Open-time analysis of the large conductance channel. (*A*) Single-channel (*middle*, calibrations: vertical = 2.0 pA; horizontal = 50 ms) and ensemble (*bottom*, calibrations: vertical = 0.5 pA; horizontal = 50 ms) traces resulting from 200-ms depolarizations from the holding potential (−90 mV) to 0 mV (*top*). Single-channel openings consisted of both brief and long open events. The ensemble (average of 140 sweeps) had a τ_{act} = 20.0 ms. (*Dotted line*) Zero current level. (*B*) Single-channel open events (825 total events) were tabulated for the 140 sweeps used to construct the ensemble in *A*. Open event durations were binned at 0.5 ms. The smooth solid line represents the best fit as the sum of two exponentials (see Table I). A two-exponential fit was better than a single-exponential fit as determined by the weighted chi-square values of 0.99 and 1.0 × 10^8, respectively.

TABLE I

Fitted Open Time Parameters*

Voltage	ω_1	τ_1	ω_2	τ_2
mV		*ms*		*ms*
−10	30.8 ± 13.2	3.4 ± 1.2	36.8 ± 16.1	21.3 ± 5.9
	(6)	(6)	(6)	(6)
0	90.4 ± 30.1	2.2 ± 0.4	89.8 ± 19.5	28.5 ± 8.0
	(9)	(9)	(9)	(9)
10	58.0 ± 19.7	2.1 ± 0.4	122.2 ± 25.9	50.0 ± 24.8
	(6)	(6)	(6)	(6)
20	213.3 ± 124	2.8 ± 0.4	127.0 ± 30.2	33.3 ± 9.4
	(6)	(6)	(6)	(6)

*Data are for cell-attached patches with ≤4 channels in each patch. However, even for multichannel patches, only openings from baseline to a single open level were measured, binned (at 0.5 ms), and fit by the following double exponential equation: $Y = (\omega_1/\tau_1) \exp\{-t/\tau_1\} + (\omega_2/\tau_2) \exp\{-t/\tau_2\}$, where t is the center time value of a given bin and ω_1 and ω_2 are the weights of the time constants τ_1 and τ_2, respectively. The number of experiments are shown in parentheses.

increased maximum L current conductance (G_{max}) 2.6-fold and accelerated τ_{act} 3.7-fold (at 20 mV). The acceleration of macroscopic L current under the single-channel recording conditions was seen at all voltages (Fig. 8 B). Moreover, under these conditions L current activates with a time constant (~20 ms) nearly identical to that seen for ensembles of the 14-pS channel. Fig. 10 A illustrates the G-V relationships recorded under control conditions (○) and in the presence of 110 mM BaCl$_2$ +
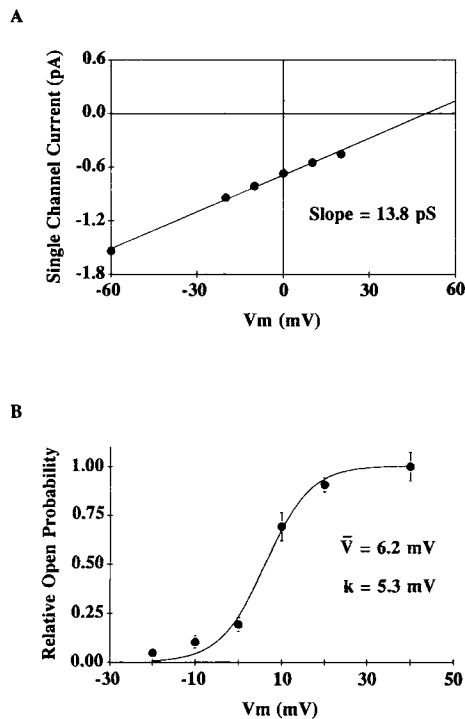

FIGURE 7. Voltage dependence of the large conductance calcium channel. (A) Average single-channel current versus voltage relationship tabulated from a total of 11 different patches with each patch containing up to four channels. Standard errors are smaller than symbol size. Typically, depolarizations to potentials ≥ −20 mV were required to elicit openings of the high-conductance channel. A linear regression of the data (R^2 = 0.9956) revealed a single-channel conductance of 13.8 pS. (B) Average relative open probability versus voltage relationship of the large conductance channel. P_0 was calculated and normalized as described in Methods. The normalized values of P_0 were then averaged and fitted according to the Boltzmann relationship: $P_0/P_{0(max)} = 1/[1 + \exp{(V_{P0.5} - V)/k_P}]$, where $P_{0(max)}$ is the maximum P_0, $V_{P0.5}$ is the potential that elicits half maximal P_0, V is the test potential, and k_P is a slope factor. The smooth solid line represents the Boltzmann fit to the data with values of $V_{P0.5}$ = 6.2 mV, k_P = 5.3 mV, and R^2 = 0.9965.

5 μM Bay K 8644 (●). Both G-V relationships were well fitted by a single Boltzmann distribution. The single-channel recording conditions caused a ~7 mV hyperpolarizing shift in the G-V curve without a significant effect on the slope factor (Fig. 10 A and Table II).

Effect of Single-Channel Recording Conditions on Charge Movement

Cultured skeletal muscle myotubes exhibit an immobilization-resistant intramembrane charge movement that triggers SR calcium release (Adams et al., 1990; García and Beam, 1994) and has been suggested to be associated with voltage-dependent conformational changes in the skeletal muscle DHPR that precede channel opening

(García et al., 1994). Thus, because skeletal muscle DHPRs are thought to give rise to both L current and immobilization-resistant intramembrane charge movement, we also tested the effect of our single-channel recording conditions on intramembrane charge movement (Figs. 9 and 10 *B*).

Under control conditions, there was near equality of Q_{on} and Q_{off} at all potentials (Fig. 9, *left*), indicating that the addition of 0.5 mM $CdCl_2$ + 0.2 mM $LaCl_3$ adequately blocked L current. Under the single-channel recording conditions, ionic current during the pulse was completely blocked, but a component of unblocked ionic tail current remained upon repolarization (Fig. 9, *right*). Nevertheless, Q_{on}
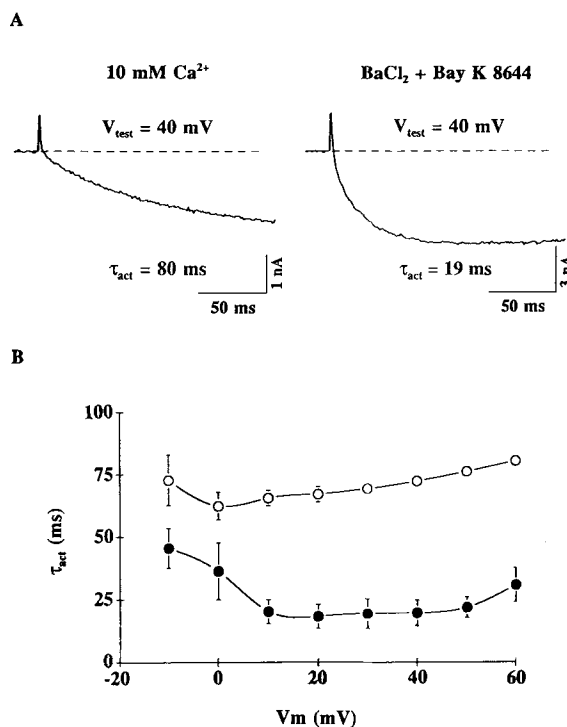
A

10 mM Ca^{2+}

V_{test} = 40 mV

τ_{act} = 80 ms

50 ms

BaCl₂ + Bay K 8644

V_{test} = 40 mV

τ_{act} = 19 ms

50 ms

B

FIGURE 8. Effect of single-channel recording conditions on the activation of macroscopic L current. (*A*) Macroscopic L current was recorded with the whole-cell patch clamp technique and activation was fit by a single exponential function as described in Methods. With 10 mM Ca^{2+} as the charge carrier (*left*), a 200-ms depolarization to 40 mV elicited a slowly developing inward current that had a τ_{act} = 80 ms. Exchange of the control recording solution for one containing 110 mM BaCl₂ + 5 μM Bay K 8644 caused a 327% increase in peak current (5.92 nA vs 1.81 nA). In addition, this exchange accelerated the activation time constant (from 80 to 19 ms). On average, τ_{act} was accelerated ~3.7-fold (19.6 ms vs 72.3 ms) at 40 mV. Data shown are for cell C73 (capacitance = 208 pF). (*B*) The τ_{act} under control (10 Ca^{2+}) or single-channel recording conditions (110 mM BaCl₂ + 5 μM Bay K 8644) is plotted versus voltage. The single-channel recording conditions accelerated τ_{act} at all voltages.

appears to be an adequate measure of charge movement under these conditions because Q_{on} saturates at strong depolarizations (Fig. 10 *B*, ●). The data shown in Fig. 9 indicate that the single-channel recording conditions do not greatly alter either the kinetics or total amount of immobilization-resistant intramembrane charge movement. Moreover, under both control and single-channel conditions, the voltage dependence of conductance is steeper than that of charge movement. Nevertheless, the single-channel recording conditions caused opposite shifts in the *G-V* and

intramembrane charge movement versus voltage $(Q\text{-}V)$ relationships (Fig. 10 and Table II).

DISCUSSION

Single-Channel Behavior of Skeletal T Current

The present results represent the first characterization of unitary activity of voltage-dependent calcium channels in native skeletal muscle. The major finding described here is that in developing mouse skeletal muscle the unitary activity of a 9-pS channel and a 14-pS channel reproduce the majority of macroscopic behavior of T current
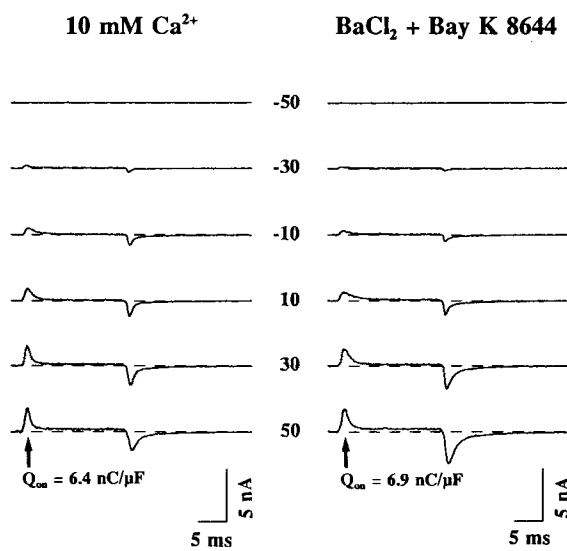

FIGURE 9. Effect of single-channel recording conditions on intramembrane charge movement. Intramembrane charge movement resulting from 20-ms depolarizations to the indicated potentials was measured in the presence of 0.5 mM Cd^{2+} and 0.2 mM La^{3+} under control conditions (*left;* 10 Ca^{2+}) and after changing to the single-channel recording solution (*right;* 110 mM $BaCl_2$ + 5 μM Bay K 8644). In the presence of 110 mM $BaCl_2$ + 5 μM Bay K 8644, a small amount of ionic tail current typically remained upon repolarization. However, the charge moved in the outward direction upon depolarization (Q_{on}) was an adequate measure of intramembrane charge movement under both control and single-channel recording conditions. For comparison, the value of Q_{on} at 50 mV in each condition is shown below the appropriate trace. From 11 experiments, $Q_{on(max)}$ was 7.2 ± 0.5 nC/μF in control and 8.0 ± 0.6 nC/μF in the presence of 110 mM $BaCl_2$ + 5 μM Bay K 8644. Data shown were obtained from cell C91 (capacitance = 481 pF).

and L current, respectively. Similar to T current, the 9-pS channel activates at potentials 20–30 mV more hyperpolarized than macroscopic L current and the 14-pS channel, inactivates rapidly in a voltage-dependent manner, and is insensitive to DHPs. These properties are similar to those reported for T-type channels in a variety of other tissues including guinea pig ventricular myocytes (Nilius et al., 1985), chick sensory neurones (Fox et al., 1985), and GH_3 pituitary cells (Armstrong and Eckert, 1987). Thus, this study demonstrates that in developing skeletal muscle, the unitary behavior of the 9-pS channel accounts for macroscopic T current and closely resembles T-type calcium current observed in other tissue.

Single-Channel Behavior of Skeletal L Current

A second class of calcium channels, distinct from the that arising from the 9-pS channel, were also identified in our single-channel experiments. These channels exhibited a larger single-channel conductance (14 pS), produced slowly activating, DHP-sensitive, ensemble currents positive to −10 mV, and displayed little inactiva-
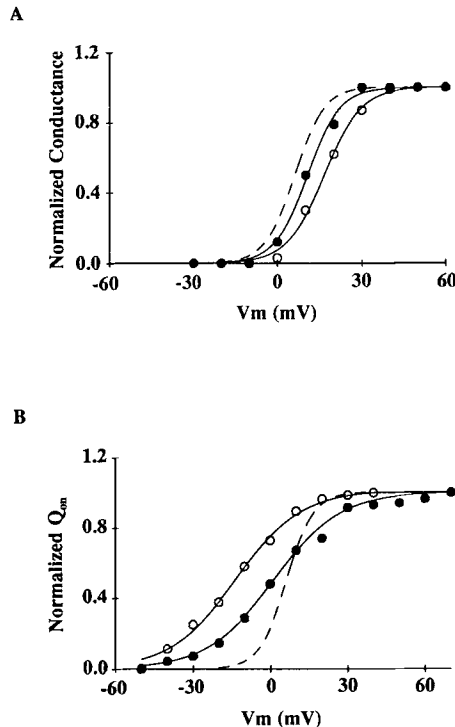
A

B

FIGURE 10. Effect of single-channel recording conditions on the voltage dependence of macroscopically recorded conductance (*A*) and intramembrane charge movement (*B*). In both *A* and *B*, the Gaussian fit of the P_0-V data shown in Fig. 7 *B* is plotted in dashed lines for comparison. Conductance data were obtained from 200-ms depolarizations to the indicated potentials in control solution (10 Ca^{2+} − ○) or after exchange for the single-channel recording solution (110 mM BaCl$_2$ + 5 μM Bay K 8644 − ●). To obtain calcium conductance, peak *i*-*V* data were fitted by the following equation to determine the reversal potential (V_{rev}): $I = G_{max}\cdot(V - V_{rev})/[1 + \exp\{(V_{G0.5} - V)/k_G\}]$, where G_{max} is the maximal conductance and $V_{G0.5}$ is the potential at which half maximal conductance is activated, *V* is the test potential, and k_G is a slope factor. Values of conductance were then calculated as $G_{Ca}(V) = I_{Ca}/(V - V_{rev})$ and normalized to G_{max}. Finally, the normalized values of G_{Ca} were fitted (*smooth solid lines*) according to $G_{Ca}(V)/G_{max} = 1/[1 + \exp\{(V_{G0.5} - V)/k_G\}]$. The $V_{G0.5}$ and k_G parameters are 17 and 6.3 mV in control (○) and 10 mV and 4.3 mV in the presence of 110 mM BaCl$_2$ + 5 μM Bay K 8644 (●). Data shown are for cell B90 (capacitance = 68 pF). (*B*) Charge movement data were obtained from 20-ms depolarizations to the indicated potentials in control solution (○) or after exchange for the single-channel recording solution (●). Values of *Q* were determined by integrating the "ON" outward transient (Q_{on}) at each potential (*V*), normalized by the maximal value (Q_{max}), and fitted according to: $Q/Q_{max} = 1/[1 + \exp\{(V_{Q0.5} - V)/k_Q\}]$, where $V_{Q0.5}$, *V*, and k_Q have their usual meanings with regard to charge movement. The $V_{Q0.5}$ and k_Q parameters were −13.4 and 12.8 mV in control (○) and 1.2 and 13.0 mV in the presence of 110 mM BaCl$_2$ + 5 μM Bay K 8644 (●). Data shown are for cell C89 (capacitance = 625 pF).

tion. These properties are similar to slow calcium current recorded macroscopically in skeletal muscle under identical recording conditions. Thus, the time-averaged behavior of the 14-pS channel represents the single-channel correlate of L current in skeletal muscle.

The macroscopic properties of L current in skeletal muscle are distinct from DHP-sensitive calcium current seen in other tissues. For example, skeletal muscle L current activates ~20 times more slowly than cardiac (Nilius et al., 1985; Tanabe, Adams, Numa, and Beam, 1991), secretory (Armstrong and Eckert, 1987), or neuronal (Fox et al., 1985) L-type calcium current. In addition, skeletal L current activates over a more depolarized range than other DHP-sensitive calcium currents (Adams et al., 1990). Moreover, unlike DHP-sensitive calcium currents from other tissues, skeletal L current is produced by a channel protein that is thought to function as a voltage sensor that couples membrane depolarization to SR calcium release (Ríos and Brum, 1987; García and Beam, 1994). Skeletal L-type calcium channels are also different in that they have been reported to conduct magnesium (Almers and Palade, 1981). Finally, the skeletal DHPR displays only 66 and 64% overall identity with the cardiac (Mikami, Imoto, Tanabe, Niidome, Mori, Takeshima, Narumiya, and Numa, 1989) and neuronal (Williams, Feldman, McCue, Brenner, Velicelebi, Ellis, and

TABLE II

Average Values of Fitted Parameters in Control and Single-Channel Solutions

Recording solution	GV data			QV data			G_{max}/Q'_{max} [‡]
	G_{max}	$V_{G0.5}$	k_G	Q_{max}	$V_{Q0.5}$	k_Q	
	nS/nF	mV	mV	$nC/\mu F$	mV	mV	nS/pC
10 mM Ca^{2+}	354 ± 24	14.0 ± 1.2	6.0 ± 0.2	7.2 ± 0.5	−5.0 ± 3.0	13.2 ± 0.7	75
	(16)	(16)	(16)	(11)	(11)	(11)	
110 mM $BaCl_2$ +	925 ± 222*	7.0 ± 5.9	5.6 ± 0.6	8.0 ± 0.6	7.8 ± 2.2	13.9 ± 0.5	168
5 μM Bay K 8644	(5)	(5)	(5)	(11)	(10)	(10)	

*Data shown are for myotubes with a maximum estimated series resistance error ≤ 10 mV (average of 8.2 ± 0.5 mV). The number of experiments are shown in parentheses. Values were calculated as described in the legend to Fig. 10. [‡]Q'_{max} is a measure of intramembrane charge movement associated with I_{slow} and is calculated as the difference between Q_{max} and the maximum amount of charge movement in mouse dysgenic myotubes (~2.5 nC/μF; Adams et al., 1990). For comparison, fitted parameters for the voltage dependence of P_0 were: $V_{P0.5}$ = 6.2 mV and k_P = 5.3 mV.

Harpold, 1992) L-type channels, respectively. Thus, it is reasonable to believe that the unitary behavior of L current should differ from that of other DHP-sensitive calcium channels.

Unfortunately, until now it has not been possible to study the unitary behavior of DHP-sensitive calcium channels functioning in native skeletal muscle. Thus, unitary activity due to the skeletal muscle DHPR could only be studied in detail in reconstituted systems. Although initial studies on the skeletal muscle channel in bilayers reported a single conductance level (Affolter and Coronado, 1985; Flockerzi et al., 1986), subsequent reports have described several distinct subconductance states. For example, using purified rabbit T tubule membranes incorporated into planar lipid bilayers, three different groups have similarly demonstrated three different conductance states (~3, 9, and 12 pS) of the skeletal muscle DHP-sensitive calcium channel (Ma and Coronado, 1988; Yatani et al., 1988; Mejía-Alvarez et al., 1991). However, each study reported a different conductance level corresponding to

the primary or longest mean lifetime. In addition, two conductance states (12–14 pS and 22-pS) that also appear to correspond to two substates of the same channel, have been reported using purified rabbit skeletal muscle DHPRs incorporated into planar lipid bilayers (Smith et al., 1987). Multiple subconductance states have also been reported for DHPRs purified from guinea pig skeletal muscle incorporated into planar bilayers (Hymel et al., 1989).

Unitary activity of DHP-sensitive calcium channels, presumably representing the skeletal muscle L-type channel, has also been recorded from BC_3H1 (Caffrey et al., 1987) and C2 (Lansman, 1990; Winegar and Lansman, 1990) cells, two clonal cell lines derived from skeletal muscle. These studies, like the present work on native muscle, found a single unitary conductance (12–16 pS) and no other significant conductance states. Thus, for the skeletal L-type calcium channel, subconductance behavior has been consistently reported in cell-free bilayer experiments, whereas experiments on intact cells describe a single conductance state. Therefore, the disparity within the literature between the presence or absence of subconductance states appears to be a consequence of the difference in channel environments between cell and bilayer experiments. For example, purification and incorporation of the channel into artificial bilayers might disrupt association of subunits, interactions with modulators (kinases/G-proteins), or destabilize the native conformation. Clearly, the environment in a bilayer is considerably different from that in the cell, where DHP receptors are thought to be precisely arranged as junctional tetrads that communicate with ryanodine receptors (Block et al., 1988; Takekura et al., 1994). The regular morphological arrangement of the L-type calcium channel in skeletal muscle, as well as its interaction with cellular regulatory mechanisms, may stabilize a single conducting state of the open channel.

Comparison of Single-Channel and Macroscopic Behavior

Bilayer experiments on the skeletal muscle L-type channel have found that the single channel P_0-V relationship (Ma et al., 1991; Mejía-Alvarez et al., 1991) is shifted 15–25 mV hyperpolarized compared to the whole cell G-V relationship (Mejía-Alvarez et al., 1991). Though not directly tested, this discrepancy was ascribed to differences in either recording conditions or lipid environments in whole-cell and bilayer experiments. The present work demonstrates that the unitary P_0-V and macroscopic G-V relationships are in reasonably good agreement, when activity of the channels are monitored under identical lipid and recording environments. Under single-channel recording conditions, the P_0-V, G-V, and Q-V curves all had similar midpoint voltages $(V_{0.5})$ of activation (6.2, 7.0, and 7.8 mV, respectively). However, the steepness factor (k) of the P_0-V relationship (5.3 mV) more closely resembles that of the G-V relationship (5.6 mV) than the shallower voltage dependence of intramembrane charge movement (13.9 mV). This result supports the model proposed by García et al. (1994) suggesting that voltage-dependent transitions of the skeletal muscle DHPR that give rise to intramembrane charge movement are distinct from transitions that result in channel opening, and consequently, conductance. Finally, consistent with an increase in P_0, the single-channel recording conditions produced a

more than twofold increase in the ratio of G_{max}/Q'_{max} (Adams et al., 1990) without a change in the number of functional channels (because Q'_{max} was unaltered).

One surprising effect caused by the single-channel recording solution is an opposite shift in the macroscopic $G-V$ and $Q-V$ relationships: a 7-mV hyperpolarizing shift in the $G-V$ relationship and a 13-mV depolarizing shift in the $Q-V$ relationship (Fig. 10 and Table II). Previous work has shown that the voltage dependence of intramembrane charge movement in skeletal muscle is shifted by alterations in extracellular divalent ion concentrations (García, McKinley, Appel, and Stefani, 1992), but is not significantly altered by DHP agonists (Lamb and Walsh, 1987). Thus, the depolarizing shift of the $Q-V$ relationship produced by the single-channel recording solution can be explained by the change in extracellular divalents (~ 10 mM Ca^{2+} to ~ 110 mM Ba^{2+}). The $G-V$ relationship of L-type channels has been shown to be shifted negatively by both DHP agonists (Sanguinetti, Krafte, and Kass, 1986) and equimolar substitution of Ba^{2+} for Ca^{2+} (Tanabe, Mikami, Numa, and Beam, 1990), and positively by increases in extracellular divalent concentration (Donaldson and Beam, 1983). Series resistance errors associated with increased current amplitude would also tend to cause a negative shift. Thus, the smaller negative shift in the $G-V$ relationship produced by the single-channel recording conditions represents a balance between these effects. In any case, the opposite shift in the $G-V$ and $Q-V$ relationships is consistent with the idea (García et al., 1994) that the voltage-dependent transition dominating channel opening is distinct from the transitions generating measured charge movement. Under such a scheme, the depolarizing shift of the $G-V$ relationship may involve an effect of the single-channel recording conditions on a voltage-dependent transition that is too slow in skeletal muscle to be reflected in measurements of charge movement.

In summary, our experimental results on single-channel and macroscopic currents reveal that: (a) developing mouse skeletal muscle contains two distinct voltage-dependent calcium channels determined from single-channel analysis: a low conductance (9 pS) and a DHP-sensitive high conductance (14 pS) channel that correspond to T current and L current, respectively; (b) the DHP-sensitive calcium channel exhibits a single conductance state in native muscle; and (c) the activation of L current has a voltage dependence more closely resembling that of P_0 than that of intramembrane charge movement.

REFERENCES

Adams, B. A., and K. G. Beam. 1989. A novel calcium current in dysgenic skeletal muscle. *Journal of General Physiology.* 94:429–444.

Adams, B. A., T. Tanabe, A. Mikami, S. Numa, and K. G. Beam. 1990. Intramembrane charge movement restored in dysgenic skeletal muscle by injection of dihydropyridine receptor cDNAs. *Nature.* 346:569–572.

Affolter, H., and R. Coronado. 1985. Agonists Bay-K8644 and CGP-28392 open calcium channels reconstituted from skeletal muscle transverse tubules. *Biophysical Journal.* 48:341–347.

Almers, W., and P. T. Palade. 1981. Slow calcium and potassium currents across frog muscle membrane: measurements with a vaseline-gap technique. *Journal of Physiology.* 312:159–176.

Armstrong, D., and R. Eckert. 1987. Voltage-activated calcium channels that must be phosphorylated to respond to membrane depolarization. *Proceedings of the National Academy of Sciences, USA.* 84:2518–2522.

Arreola, J., J. Calvo, M. C. García, and J. A. Sanchez. 1987. Modulation of calcium channels of twitch skeletal muscle fibres of the frog by adrenaline and cyclic adenosine monophosphate. *Journal of Physiology.* 393:307–330.

Beam, K. G., C. M. Knudson, and J. A. Powell. 1986. A lethal mutation in mice eliminates the slow calcium current in skeletal muscle cells. *Nature.* 320:168–170.

Beam, K. G., and C. M. Knudson. 1988a. Calcium currents in embryonic and neonatal mammalian skeletal muscle. *Journal of General Physiology.* 91:781–798.

Beam, K. G., and C. M. Knudson. 1988b. Effects of postnatal development on calcium currents and slow charge movement in mammalian skeletal muscle. *Journal of General Physiology.* 91:799–815.

Block, B. A., T. Imagawa, K. P. Campbell, and C. Franzini-Armstrong. 1988. Structural evidence for direct interaction between the molecular components of the transverse tubule/sarcoplasmic reticulum junction in skeletal muscle. *Journal of Cell Biology.* 107:2587–2600.

Caffrey, J. M., A. M. Brown, and M. D. Schneider. 1987. Mitogens and oncogenes can block the induction of specific voltage-gated ion channels. *Science.* 236:570–573.

Cavalié, A., D. Pelzer, and W. Trautwein. 1986. Fast and slow gating behavior of single calcium channels in cardiac cells. *Pflügers Archiv.* 406:241–258.

Chandler, W. K., R. F. Rakowski, and M. F. Schneider. 1976. Effects of glycerol treatment and maintained depolarization on charge movement in muscle. *Journal of Physiology.* 254:285–316.

Cognard, C., M. Lazdunski, and G. Romey. 1986a. Different types of Ca^{2+} channels in mammalian skeletal muscle cells in culture. *Proceedings of the National Academy of Sciences, USA.* 83:517–521.

Cognard, C., G. Romey, J.-P. Galizzi, M. Fosset, and M. Lazdunski. 1986b. Dihydropyridine-sensitive Ca^{2+} channels in mammalian skeletal muscle cells in culture: electrophysiological properties and interactions with Ca^{2+} channel activator (Bay K8644) and inhibitor (PN 200-110). *Proceedings of the National Academy of Sciences, USA.* 83:1518–1522.

Cota, G., and E. Stefani. 1986. A fast-activated inward calcium current in twitch muscle fibres of the frog (*Rana montezume*). *Journal of Physiology.* 370:151–163.

Dirksen, R. T., and K. G. Beam. 1994. Comparison of whole-cell and single-channel properties of the skeletal muscle slow calcium channel. *Biophysical Journal.* 66:A129. (Abstr.)

Dirksen, R. T., T. Tanabe, and K. G. Beam. 1993. Single channel analysis of native and expressed skeletal muscle calcium channels. *Biophysical Journal.* 64:A6. (Abstr.)

Donaldson, P. L., and K. G. Beam. 1983. Calcium currents in fast-twitch skeletal muscle of the rat. *Journal of General Physiology.* 82:449–468.

Flockerzi, V., H.-J. Oeken, F. Hofmann, D. Pelzer, A. Cavalié, and W. Trautwein. 1986. Purified dihydropyridine-binding site from skeletal muscle t-tubules is a functional calcium channel. *Nature.* 323:66–68.

Fosset, M., E. Jaimovitch, E. Delpont, and M. Lazdunski. 1983. [^{3}H]Nitrendipine receptors in skeletal muscle. Properties and preferential localization in transverse tubules. *Journal of Biological Chemistry.* 258:6086–6092.

Fox, A. P., M. C. Nowycky, and R. W. Tsien. 1987. Single-channel recordings of three types of calcium channels in chick sensory neurones. *Journal of Physiology.* 394:173–200.

Franco, A. Jr., and J. B. Lansman. 1990a. Calcium entry through stretch-inactivated ion channels in *mdx* myotubes. *Nature.* 344:670–673.

Franco, A. Jr., and J. B. Lansman. 1990b. Stretch-sensitive channels in developing muscle cells from a mouse cell line. *Journal of Physiology.* 427:361–380.

Franzini-Armstrong, C., M. Pincon-Raymond, and F. Rieger. 1991. Muscle fibers from dysgenic mouse *in vivo* lack a surface component of peripheral couplings. *Developmental Biology.* 146:364–376.

García, J., and K. G. Beam. 1994. Measurement of calcium transients and slow calcium current in myotubes. *Journal of General Physiology.* 103:107–123.

García, J., K. McKinley, S. H. Appel, and E. Stefani. 1992. Ca^{2+} current and charge movement in adult single human skeletal muscle fibres. *Journal of Physiology.* 454:183–196.

García, J., T. Tanabe, and K. G. Beam. 1994. Relationship of calcium transients to calcium currents and charge movements in myotubes expressing skeletal and cardiac dihydropyridine receptors. *Journal of General Physiology.* 103:125–147.

Gonoi, T., and S. Hasegawa. 1988. Post-natal disappearance of transient calcium channels in mouse skeletal muscle: effects of denervation and culture. *Journal of Physiology.* 401:617–637.

Hamill, O. P., A. Marty, E. Neher, B. Sakmann, and F. J. Sigworth. 1981. Improved patch-clamp techniques for high-resolution current recording from cells and cell-free membrane patches. *Pflügers Archiv.* 391:85–100.

Hymel, L., J. Striessing, H. Glossmann, and H. Schindler. 1988. Purified skeletal muscle 1,4-dyhydropyridine receptor forms phosphorylation-dependent oligomeric calcium channels in planar bilayers. *Proceedings of the National Academy of Sciences, USA.* 85:4290–4294.

Lamb, G. D., and T. Walsh. 1987. Calcium currents, charge movement and dihydropyridine binding in fast- and slow-twitch muscles of rat and rabbit. *Journal of Physiology.* 393:595–617.

Lansman, J. B. 1990. Blockade of current through single calcium channels by trivalent lanthanide cations. *Journal of General Physiology.* 95:679–696.

Ma, J., and R. Coronado. 1988. Heterogeneity of conductance states in calcium channels of skeletal muscle. *Biophysical Journal.* 53:387–395.

Ma, J., C. Mundiña-Weilenmann, M. M. Hosey, and E. Ríos. 1991. Dihydropyridine-sensitive skeletal muscle Ca channels in polarized planar bilayers. 1. Kinetics and voltage dependence of gating. *Biophysical Journal.* 60:890–901.

Mejía-Alvarez, R., M. Fill, and E. Stefani. 1991. Voltage-dependent inactivation of T-tubular skeletal calcium channel in planar lipid bilayers. *Journal of General Physiology.* 97:393–412.

Mikami, A., K. Imoto, T. Tanabe, T. Niidome, Y. Mori, H. Takeshima, S. Narumiya, and S. Numa. 1989. Primary structure and functional expression of the cardiac dihydropyridine-sensitive calcium channel. *Nature.* 340:230–233.

Nilius, B., P. Hess, J. B. Lansman, and R. W. Tsien. 1985. A novel type of cardiac calcium channel in ventricular cells. *Nature.* 316:443–446.

Parent, L., M. Gopalakrishnan, A. E. Lacerda, and A. M. Brown. 1994. Inactivation of skeletal-cardiac calcium channel chimeras. *Biophysical Journal.* 66:A230. (Abstr.)

Perez-Reyes, E., H. S. Kim, A. E. Lacerda, W. Horne, X. Wei, D. Rampe, K. P. Campbell, A. M. Brown, and L. Birnbaumer. 1989. Induction of calcium currents by the expression of the α_1-subunit of the dihydropyridine receptor from skeletal muscle. *Nature.* 340:233–236.

Ríos, E., and G. Brum. 1987. Involvement of dihydropyridine receptors in excitation-contraction coupling in skeletal muscle. *Nature.* 325:717–720.

Sanguinetti, M. C., D. S. Krafte, and R. S. Kass. 1986. Voltage-dependent modulation of calcium channel current in heart cells by Bay K8644. *Journal of General Physiology.* 88:369–392.

Sculptoreanu, A., T. Scheuer, and W. A. Catterall. 1993. Voltage-dependent potentiation of L-type Ca^{2+} channels due to phosphorylation by cAMP-dependent protein kinase. *Nature.* 364:240–243.

Smith, J. S., E. J. McKenna, J. Ma, J. Vilven, P. L. Vaghy, A. Schwartz, and R. Coronado. 1987. Calcium channel activity in a purified dihydropyridine-receptor preparation of skeletal muscle. *Biochemistry.* 26:7182–7188.

Takekura, H., L. Bennett, T. Tanabe, K. G. Beam, and C. Franzini-Armstrong. 1994. Restoration of junctional tetrads in dysgenic myotubes by dihydropyridine receptor cDNA. *Biophysical Journal.* 67:793–803.

Tanabe, T., A. Mikami, S. Numa, and K. G. Beam. 1990. Cardiac-type excitation-contraction coupling in dysgenic muscle injected with cardiac dihydropyridine receptor cDNA. *Nature.* 344:451–453.

Tanabe, T., B. A. Adams, S. Numa, and K. G. Beam. 1991. Repeat I of the dihydropyridine receptor is critical in determining calcium channel activation kinetics. *Nature.* 352:800–803.

Wellner, M.-C., and G. Isenberg. 1993. Properties of stretch-activated channels in myocytes from the guinea-pig urinary bladder. *Journal of Physiology.* 466:213–227.

Williams, M. E., D. H. Feldman, A. F. McCue, R. Brenner, G. Velicelebi, S. B. Ellis, and M. M. Harpold. 1992. Structure and functional expression of α_1, α_2, and β subunits of a novel human neuronal calcium channel subtype. *Neuron.* 8:71–84.

Winegar, B. D., and J. B. Lansman. 1990. Voltage-dependent block by zinc of single calcium channels in mouse myotubes. *Journal of Physiology.* 425:563–578.

Yatani, A., Y. Imoto, J. Codina, S. L. Hamilton, A. M. Brown, and L. Birnbaumer. 1988. The stimulatory G protein of adenylyl cyclase, G_s, also stimulates dihydropyridine-sensitive calcium channels. *Journal of Biological Chemistry.* 263:9887–9895.